https://doi.org/10.5194/nhess-2019-240
Preprint. Discussion started: 18 September 2019

Natural Hazards and Earth System Sciences
Discussions

Shape and dimension estimations of landslide rupture zones via correlations of characteristic parameters

Gisela Domej [1]
Céline Bourdeau [1]
Luca Lenti [1]
Salvatore Martino [2]

[1] IFSTTAR / GERS / Sols, Roches et Ouvrages Géotechniques / 14–20 Boulevard Newton / 77447 Marne–la–Vallée, France
[2] Università di Roma / CERI & Dipartimento di Scienze della Terra / Piazzale Aldo Moro 5 / 00185 Rome, Italy

Corresponding author: gisela.domej@ifsttar.fr

Abstract

For many geotechnical purposes, the proper estimation of shapes and dimensions of landslide rupture zones is of significant importance. Very often this exact delineation is difficult due to the lack of information on rupture zone extents in 3D. Based on a global landslide inventory, this study presents a refined statistical analysis correlating dimension-related and shape-related parameters characterizing a rupture zone in 3D to its volume. Dimension-parameters are approximated by linear regressions increasing with greater volumes, whereas shape-related parameters appear stable throughout the entire range of volumes. Revealing themselves as very stable, these correlations can be used, hence, to extrapolate from a distinct parameter to the volume of a landslide rupture zone. In a second stage, ratios of dimension-related parameters are correlated with rupture zone volumes. Also, this type of correlation delivers very stable results showing that ratios are constant throughout the entire range of volumes. Making use of this ratio consistency, it is possible to deduce one of the two parameters when the other one is given. This latter aspect seems to be promising for remote sensing surveys when initial rupture areas or rupture volumes should be delineated.

Keywords

landslide shape, landslide dimension, rupture zone, landslide size estimation, landslide database

1. Introduction

Across the globe, landslides are triggered by a variety of causes. They regularly lead to loss of life and damage ranging from smaller to a greater extent (Bird and Bommer, 2004; Froude and Petley, 2018). Common triggers are of tectonic, volcanic, meteorological and anthropogenic nature – or a combination of them (USGS, 2004). As an example illustrating the trail of destruction serves the landslide series triggered during Hurricane Mitch in October 1998, which caused tremendous damage and 2,000 fatalities in Nicaragua alone (Lott et al., 1999). Another more recent example of devastation is the landslide series after the Sichuan Earthquake in May 2008 with a ten times higher number of victims (20,000; Yin et al., 2009).
In view of constant population growth and expansion to new – and occasionally endangered – living environments, proper management of landslide risk is essential for social resilience.
Over the last decades, major contributions to a better understanding of the phenomenon of landslides were made by the establishment and consecutive exploration of landslide databases, which could be chronologic (i.e., listing landslides with different triggers over time) or event based (i.e., listing landslides caused by a particular triggering event). The latter might be tectonic events (e.g., earthquakes, fault ruptures or volcanic activity), meteorological events (e.g., heavy rain or storms) and climatic changes on a seasonal or long term scale (e.g., snowmelt or permafrost degradation). Scientific work based on landslide databases with respect to the type of triggering events is exhaustive, and a full overview would be beyond the scope of this publication; some examples are: studies using global, regional and event based databases of earthquake-triggered landslides by Haro and Jibson (1995, 1996), Keefer et al. (1984), Presininzi & Romeo (2000), Rodríguez et al. (1999) and Tanyaş et al. (2017); studies based on landslide databases related to climatic changes such as snowmelt (e.g. Cardinali et al., 2001) and general climate change (e.g. Schlögel et al., 2011); and studies using event based meteorological databases (e.g. Bucknam et al., 2012). An even more abundant number of studies on landslide databases became available due to the increasing reliability of remote sensing techniques which allow for rapid mapping and analyses of single landslides or landslide clusters at different scales all over the globe.
Following the essential need for assessing landslides in order to manage their danger potential properly, this work presents detailed statistical analyses focusing on expected dimensions and shapes of landslide rupture

https://doi.org/10.5194/nhess-2019-240
Preprint. Discussion started: 18 September 2019

Natural Hazards and Earth System Sciences
Discussions
Open Access
EGU

zones (Fig. 1). The main goal is neither to map landslides nor to draw conclusions on event frequencies; the purpose of these analyses is a refinement of preliminary results from a previous publication of the authors (Domej et al., 2017). Based on a newly created chronologic database comprising 277 landslides in 40 countries across the globe, Domej et al. (2017) suggest that rupture zones of landslides have a common shape even though their dimensions differ.

In the first part, this publication revisits the landslide inventory by Domej et al. (2017) in order to summarize its content, main objectives, and results. The second part is dedicated to refined statistical analyses consisting of correlations between landslide volumes and single parameters characterizing landslide rupture zones and of correlations between landslide volumes and ratios of single parameters. The last section discusses results, their correspondence to Domej et al. (2017) as well as their potential fields of application.

2. Statistical analyses

As described in much more detail in Domej et al. (2017), the preliminary analyses aimed for a general understanding of the statistical behavior of geometrical parameters characterizing landslide rupture zones (Fig. 1, Table 1). The term "rupture zone" refers here to the three-dimensional landslide volume that is confined by the rupture surface at the moment of the main rupture event. In theory, i.e., if the data coverage is fully exhaustive, a total number of 66 parameters and descriptive notes with respect to longitudinal cross sections (LCS), transversal cross sections (TCS) and top views (map) are available for each landslide included in the database. However, the number of exportable parameters usually decreases due to the availability of data for one particular parameter throughout the database.

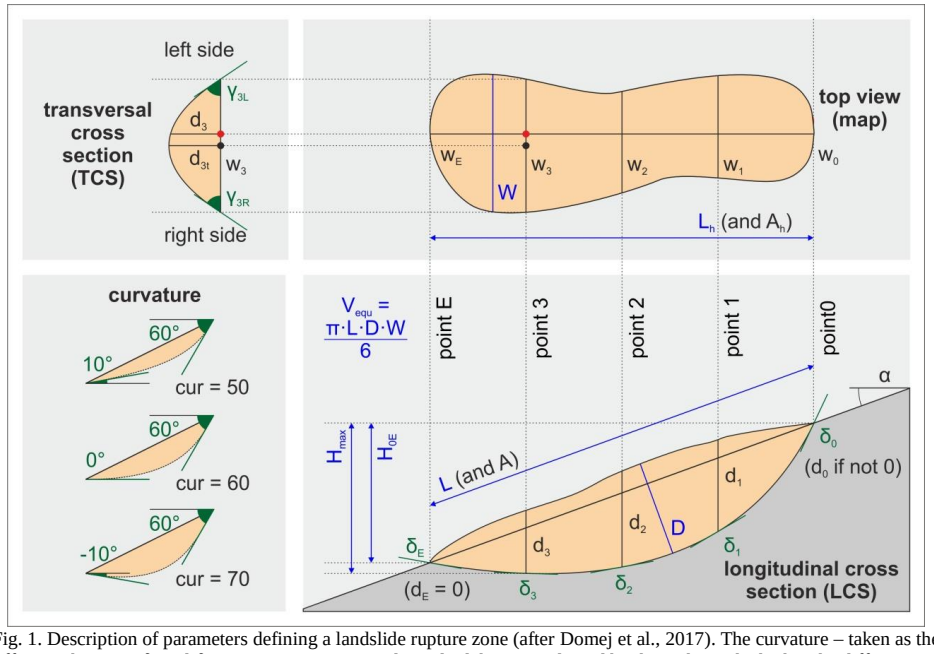

Fig. 1. Description of parameters defining a landslide rupture zone (after Domej et al., 2017). The curvature – taken as the difference between δ_0 and δ_E – is not an international standard, but was adopted by the authors; the higher the difference is, the higher is the curvature. The calculated volume (V_{equ}) is calculated by the equation of Cruden and Varnes (1996). The perspective of the TCS represents a view from the landslide toe towards the landslide crest.

Domej et al. (2017) derived average values for all parameters based on different landslide sets (i.e., the set "full" with all 277 landslides in the database, the set "SR" with all 220 landslides in seismic regions and the set "EQt" with all 99 earthquake-triggered landslides) and volume groups (i.e., 10^3–10^6 m³, 10^6–10^9 m³ and 10^9–10^{12} m³; Fig. 2a) to evaluate the overall statistical behavior of individual parameters with increasing landslide size. Independently of the three tested datasets it appeared that

- dimension-related parameters (i.e., length, width, depth, height, area, and volume) naturally increase with the volume group – thus the landslide size –, but

https://doi.org/10.5194/nhess-2019-240
Preprint. Discussion started: 18 September 2019

Natural Hazards and Earth System Sciences
Discussions
Open Access
EGU

- shape-related parameters (i.e., angles, the curvature, and ratios between distinct parameters) are almost constant for different landslide sizes.

Parameters	Description	Statistical distribution
V_{equ}	calculated volume (=(1/6) ·π·L·D·W))	increasing exponantial
A	area as reported by literature	increasing exponantial
A_h	area projected to horizontal	increasing exponantial
L	length along the slope	increasing exponantial
L_h	length projected to horizontal	increasing exponantial
H_{max}	height between point 0 and the deepest point	increasing exponantial
H_{0E}	height between point 0 and point E	increasing exponantial
W	maximum width	increasing exponantial
w_0, w_1, w_2, w_3, w_E	widths at points 0 to E	increasing exponantial
D	maximum depth	increasing exponantial
d_0, d_1, d_2, d_3, d_E	depths at points 0 to E	normal (except d_E, as it is always 0)
δ_0, δ_1, δ_2, δ_3, δ_E	angles at points 0 to E	normal
cur	curvature of the rupture surface	normal
α_{lit}	reported slope angle	normal
α_{equ}	calculated slope angle (= $\tan^{-1}(H_{0E}/L_h)$)	normal
d_{1t}, d_{2t}, d_{3t}	maximum depths of TCS I to III	(too few data; cf. argumentation in 2.1)
γ_{1L}, γ_{2L}, γ_{3L}	left flank angles of TCS I to III	
γ_{1R}, γ_{2R}, γ_{3R}	right flank angles of TCS I to III	

Table 1. Description of parameters defining a landslide rupture zone (after Domej et al., 2017). The last column indicates the type of statistical distribution of values per individual parameter throughout the database.

Although the three datasets dispose globally and independently distributed landslides characterized by different materials and triggering mechanisms, this preliminary finding is remarkable.
Nonetheless, the described approach has the drawback of different sample sizes per evaluated volume group. As indicated in Fig. 2a, all of the 42 landslides in the first volume group dispose of a maximum depth (D) over which the average is taken. For only 22 landslides, though, the reported slope angle (α_{lit}) is known. To avoid this discrepancy, and to refine results of Domej et al. (2017), the analyses presented in this publication follow the approach of simple volume–to–parameter correlation without the intermediate step of grouping according to landslide volumes (Fig. 2b). Essential to this approach is the condition that one particular landslide entry in the database stores the value for the calculated volume (V_{equ}) and the parameter to correlate (e.g., maximum depth (D)).
As mentioned in Domej et al. (2017), the choice of the calculated volume (V_{equ}) as the first correlation parameter is justified by a high recurrence throughout the database reaching 74%. Moreover, the volume of a landslide is usually considered as one of the most significant parameters relating to event magnitude and subsequent consequences (Malamud et al., 2004).

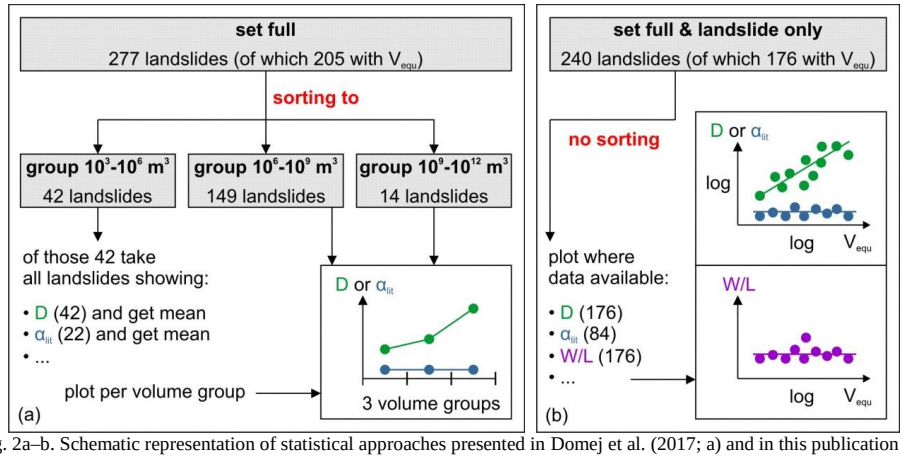

Fig. 2a–b. Schematic representation of statistical approaches presented in Domej et al. (2017; a) and in this publication (b).

https://doi.org/10.5194/nhess-2019-240
Preprint. Discussion started: 18 September 2019

Natural Hazards and Earth System Sciences
Discussions

2.1. Volume–to–parameter correlations

One of the two new approaches that allow for refined statistical analyses of the behavior of dimension- and shape-related parameters consists of volume–to–parameter correlations. One partner of correlation is necessarily the calculated volume (V_{equ}), whereas the place of the second partner is taken by any of the parameters characterizing the rupture zone in three dimensions (Fig. 1, Table 1).
Here, the choice of suitable partners of correlation is limited by reflections on sample sizes and meaningfulness. Considering the set "full/landslide only" – i.e., all classic landslides throughout the database not displaying local features of other mass movement types (Varnes, 1987) – sample sizes for different parameters vary as a function of the applied filter cascade (Table 2). Thereupon apply the filters for the two partners of correlation as uniquely those landslide records showing both the calculated volume (V_{equ}) and the respective parameter of interest can be used for evaluation (Fig. 2b). For the shape-related parameters, the calculated slope angle (α_{equ}), the angles along the rupture surface (δ_0 to δ_E) and the curvature (*cur*), the thereby obtained sample sizes are very satisfying and vary between 153 and 176 cases (second columns of Table 3a–b). The reported slope angle (α_{lit}) is to be evaluated for 84 cases, both area types – the reported area (A) and its projection to the horizontal (A_h) – are represented only by 72 cases, and all TCS related parameters are quasi non-represented by solely three cases at the maximum.

Set	Filter 1	Filter 2	Included cases
1 – "full"	-	landslide only	240
2 – "SR"	landslides in seismic regions		189
3 – "EQt"	earthquake-triggered landslides		95
4 – "full-R"	rotational landslides		76
5 – "full-T"	translational landslides		79
6 – "full-RT"	roto-translational		85

Table 2. Subsets of the database used for analyses with their respective first and second filters.

As for the reported area (A) and its projection to the horizontal (A_h), one might criticize that despite their good representation, they are not included in the volume–to–parameter correlations. Here the argument is that area reports on landslides are to be seen with caution, especially when it comes to the explicit delineation of rupture zones. Rupture and runout zones can be overlapping, adjacent, or even separated (Fig. 8a–d); very often, reported areas refer to the entire area along a slope which is affected by the sliding process. For many landslides in the database, the distinction between these different area types is not clear, and thus correlations were dismissed. Another argument is that this very uncertainty might become a field of application of the statistical correlations presented in this publication.
In contrast to the sifting of unsuitable correlation parameters, also a few new appropriate parameters were created. They might become of particular interest when delineating average dimensions of rupture zones rather than maximal possible extents in one particular location of the rupture zone.

- d_{av5}: average depth of the rupture zone below points 0, 1, 2, 3, E
- d_{av4}: average depth of the rupture zone below points 0, 1, 2, 3
- d_{av3}: average depth of the rupture zone below points 1, 2, 3
- w_{av5}: average width of the rupture zone at points 0, 1, 2, 3, E
- w_{av3}: average width of the rupture zone at points 1, 2, 3

Taking into account the finding by Domej et al. (2017), i.e., the difference in behavior between dimension- and shape-related parameters, and considering the fact that within the volume–to–parameter correlations both types of parameters exist, a homogeneous way of analyses had to be adopted. For internal consistency, all distributions of dimension-related parameters underwent the fitting of linear regressions in double-logarithmic diagrams, whereas, for all distributions of shape-related parameters, the mean value (μ) was calculated relying on the results of Domej et al. (2017), that indicate constancy of shape-related parameters throughout different volumes. Furthermore, the homogeneity of analyses between the concerned volume–to–parameter correlations and the likewise shape based volume–to–ratio correlations (next subsection) is preserved.
In the following, the analytic procedure for the most comprehensive set "full" is described. It should be mentioned beforehand, that the identical procedure was carried out also for all other sets (Table 2) in order to observe potential changes in statistical behaviors. A comparison of the results of all six tested sets is given in the discussion.
Regressions are here of the general type

$$y=\exp(b)\cdot V_{equ}\hat{}(a) \qquad \text{(Eq. 1)}$$

https://doi.org/10.5194/nhess-2019-240
Preprint. Discussion started: 18 September 2019

Natural Hazards and Earth System Sciences
Discussions

and appear in a double-logarithmic diagram as

$$\log_{10}(y)=c+a\cdot\log_{10}(V_{equ}) \quad \text{(Eq. 2)}$$

with y defining the respective parameter, a defining the gradient
and $c=\log_{10}(\exp(b))$ representing the intercept on the second axis.

Examples of regression fittings are shown in Fig. 3 for the set "full" for the maximum depth (D), the height between the point 0 and the point E (H_{0E}) and the length along the slope (L). Despite different scatter patterns, all point clouds reveal a clear increasing tendency. Regressions fit without exception with adjusted coefficients of determination (R_{adj}^2) above – or equal to – the common threshold of acceptance of 0.7 (Table 3a). Also, within the other five tested sets (Table 2) all adjusted coefficients of determination (R_{adj}^2) lie between 0.73 and 0.98. Regression fitting seems, thus, an adequate tool for correlating calculated volumes (V_{equ}) and dimension-related parameters. Results for the set "full" are listed in Table 3a. The last two columns give the constant c as well as the factor (a) that must be inserted into Eq. (2) in order to reproduce the straight line per parameter in the respective double-logarithmic diagram.

V_{equ}/…	Cases	R_{adj}^2	constant c	factor a
D	176	0.70	-0.29	0.29
d_{av5}	153	0.75	-0.65	0.29
d_{av4}	153	0.75	-0.55	0.29
d_{av3}	153	0.75	-0.46	0.30
d_0	153	d_0 contains 0, not fitted in a log-log		
d_1	153	0.72	-0.41	0.30
d_2	153	0.73	-0.37	0.29
d_3	153	0.76	-0.63	0.31
d_E	153	d_E is always 0, not fitted in a log-log		
H_{0E}	176	0.73	-0.06	0.32
H_{max}	176	0.74	-0.06	0.33
L	176	0.92	0.32	0.36
L_h	176	0.92	0.27	0.36
W	176	0.92	0.25	0.36
w_{av5}	169	0.91	0.15	0.35
w_{av3}	169	0.90	0.23	0.35
w_0	169	0.79	0.02	0.32
w_1	169	0.89	0.23	0.34
w_2	169	0.90	0.25	0.34
w_3	169	0.91	0.21	0.35
w_E	169	0.87	-0.02	0.36

Table 3a. Results for the volume–to–parameter correlations for the set "full". For all dimension-related parameters, the regression parameters (R_{adj}^2, constant c and factor a; Eq. (2)) are given.

V_{equ}/…	Cases	μ	σ	μ/σ	% in ±1σ	% in ±2σ	% in ±3σ
δ_0	153	50.37	19.41	2.59	66.0%	97.4%	100.0%
δ_1	153	18.42	14.07	1.31	66.7%	96.7%	100.0%
δ_2	153	14.83	13.93	1.06	76.5%	94.1%	98.7%
δ_3	153	10.81	11.55	0.94	82.4%	94.8%	98.7%
δ_E	153	-0.96	16.86	-0.06	73.9%	94.1%	98.0%
cur	153	51.33	25.36	2.02	70.6%	97.4%	99.4%
α_{equ}	176	17.99	11.71	1.54	71.0%	94.3%	98.9%
α_{lit}	84	19.90	13.23	1.50	73.8%	97.6%	98.8%

Table 3b. Results for the volume–to–parameter correlations for the set "full". For all shape-related parameters, the mean value (μ) with the respective standard deviation (σ) and the sampling size per sigma interval is given.

Conclusions on dispersion are to be regarded with caution in the case of dimension-related parameters. The main reason is that each point in the point clouds depends only on one value of the calculated volume (V_{equ}); i.e., there is no option to measure dispersions per distinct volume.
The procedure of analyses for shape-related parameters (Table 3b) consisted of averaging the values represented by the respective point clouds. Besides the assumption of consistency throughout different calculated volumes

https://doi.org/10.5194/nhess-2019-240
Preprint. Discussion started: 18 September 2019

Natural Hazards and Earth System Sciences
Discussions
Open Access
EGU

(V_{equ}), there is also a second strong argument favoring simple value averaging instead of regression fitting. Considering perfectly normal distributed data, certain fractions of it should lie within symmetric belts of two (μ±1σ), four (μ±2σ) and six (μ±3σ) standard deviations around the mean value. In the case of the set "full" – where the variability of the calculated volume (V_{equ}) has no impact on the statistical behaviors –, data of the individual shape-related parameters follow these suggested intervals with minor deviations (Table 3b). One can assume, hence, that data of shape-related parameters are normal distributed what emphasizes the representativeness of the respective mean value (μ). Also, the other five tested sets (Table 2) reveal very similar tendencies with respect to the required fraction of data within the three symmetric belts; only in five cases, sigma interval thresholds were missed by more than 5%.

An example of averaging values is shown in Fig. 3 for the set "full" for the calculated slope angle (α_{equ}). All mean values (μ) are listed in Table 3b, together with their standard deviations (σ) and the relations between both types of values (μ/σ) as measure for dispersion. Here, the information about dispersion is of much bigger interest than for the dimension-related parameters.

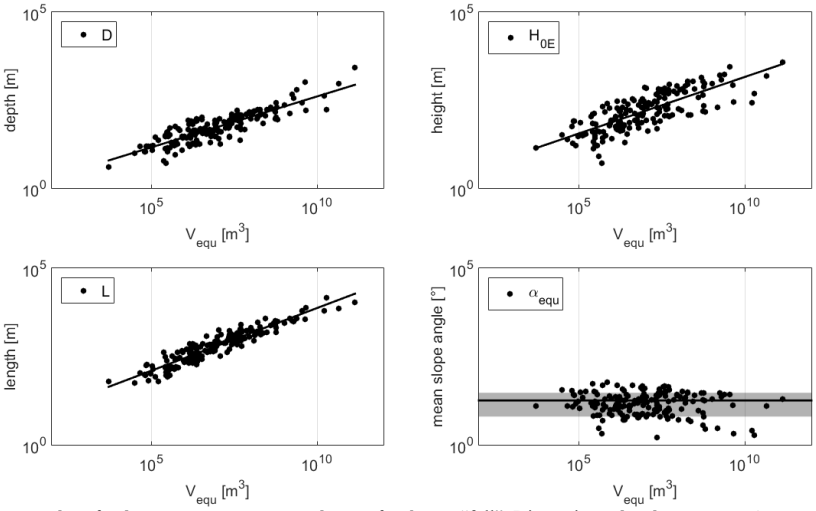

Fig. 3. Examples of volume–to–parameter correlations for the set "full". Dimension-related parameters (*D*, H_{0E}, and *L*) are approximated by a regression; for the shape-related parameter (α_{equ}) the mean value (μ) is calculated. The shading indicates the symmetric belts of two standard deviations (±1σ) around the mean value (μ).

2.2. Volume–to–ratio correlations

The second of the two new approaches designed for refined statistical analyses of the behavior of ratios consists of volume–to–ratio correlations. In agreement with Domej et al. (2017), ratios of dimension-related parameters are assumed to behave like shape-related parameters and can, therefore, be analyzed in a similar way – however, with more sophisticated filtering.

Here, the correlation partner on the second axis is a ratio of two individual – dimension-related – parameters characterizing the rupture zone in three dimensions (Fig. 1, Table 1); after adding a fifth filter (Table 2), sample sizes for the set "full" are still very high ranging from 146 to 176 (Table 4).

In analogy to the argumentation in the previous subsection, reported areas (*A*) and their projections to the horizontal (A_h) are less profitable candidates for ratios. So are separate widths (w_0 to w_E) and depths (d_0 to d_E) as they would result in specific ratios that might not be of great use for application; here, it appeared to be more promising to use the newly defined averaged parameters mentioned in the previous subsection (d_{av5}, d_{av4}, d_{av3}, w_{av5}, and w_{av3}) to create meaningful ratios.

With respect to these viewpoints and the aim of not creating ratios within the same types of dimension-related parameters (i.e., between lengths, heights, widths and depths respectively), and accounting for the difference between maximum (e.g. *W*) and average parameters (e.g. w_{av3}), 24 significant ratios were identified (Table 4).

Assuming that ratios behave statistically in the same way as other shape-related parameters, they underwent the same procedure of averaging data in order to keep the overall analyses homogeneous and comparable. Again, the basic supposition is, that ratios are constant throughout the calculated volume (V_{equ}), and the same strong argument for the representativeness of the mean value (μ) applies to the here presented volume–to–ratio correlations: Table 4 shows for the set "full" that the fractions of data lie without exception within symmetric

https://doi.org/10.5194/nhess-2019-240
Preprint. Discussion started: 18 September 2019

Natural Hazards and Earth System Sciences
Discussions

belts of two, four and six standard deviations (σ) around the mean value (μ) indicating normal distributions. Also, the other five tested sets (Table 2) reveal very similar tendencies with respect to the required fraction of data within the three symmetric belts. Only in three cases, sigma interval thresholds were missed by more than 5%.

V_{equ}/…	Cases	μ	σ	μ/σ	% in ±1σ	% in ±2σ	% in ±3σ
H_{0E}/L_h	176	0.35	0.27	1.29	82.4%	94.3%	98.3%
H_{max}/L_h	176	0.36	0.27	1.34	82.4%	94.9%	98.3%
H_{0E}/W	176	0.49	0.51	0.96	88.6%	96.0%	97.7%
H_{0E}/w_{av5}	169	0.72	0.77	0.93	88.2%	95.9%	97.6%
H_{0E}/w_{av3}	169	0.62	0.69	0.90	88.8%	95.3%	98.2%
H_{0E}/D	176	3.92	3.42	1.15	85.2%	97.7%	98.3%
H_{0E}/d_{av5}	153	7.85	5.84	1.34	85.0%	93.5%	97.4%
H_{0E}/d_{av4}	153	6.28	4.67	1.34	85.0%	93.5%	97.4%
H_{0E}/d_{av3}	153	4.87	3.62	1.35	83.7%	94.8%	97.4%
D/L	176	0.11	0.09	1.31	81.3%	90.3%	99.4%
d_{av5}/L	153	0.05	0.03	1.46	75.8%	94.1%	99.4%
d_{av4}/L	153	0.06	0.04	1.45	75.8%	94.1%	99.4%
d_{av3}/L	153	0.08	0.06	1.45	74.5%	94.1%	99.4%
W/L	176	1.17	1.38	0.85	92.1%	97.2%	97.7%
w_{av5}/L	169	0.82	0.90	0.91	89.9%	97.0%	98.2%
w_{av3}/L	169	0.95	1.01	0.95	91.1%	97.0%	98.2%
D/W	176	0.15	0.14	1.02	89.2%	94.3%	97.2%
D/w_{av5}	169	0.21	0.19	1.10	87.0%	94.7%	97.6%
D/w_{av3}	169	0.17	0.16	1.07	88.2%	95.3%	98.8%
d_{av5}/W	153	0.07	0.08	0.89	92.8%	97.4%	97.4%
d_{av4}/W	153	0.09	0.10	0.89	92.8%	97.4%	97.4%
d_{av3}/W	153	0.11	0.13	0.89	92.8%	97.4%	98.0%
d_{av5}/w_{av5}	146	0.10	0.10	0.92	94.5%	98.6%	98.6%
d_{av3}/w_{av3}	146	0.13	0.16	0.84	93.8%	98.6%	98.6%

Table 4. Results for volume–to–ratio correlations for the set "full". For all shape-related parameters (i.e., here the ratios), the mean value (μ) with the respective standard deviation (σ) and the sampling size per sigma interval is given.

Examples for averaging values are shown in Fig. 4 for the set "full" for the ratio of the height between the point 0 and the point E to the projected length (H_{0E}/L_h), the ratio of the average depth to the length along the slope (d_{av5}/L), the ratio of the average width to the length along the slope (w_{av5}/L) and the ratio of the average depth to the average width (d_{av5}/w_{av5}). The corresponding mean values (μ) – as well as those of the other 20 ratios – are listed in Table 4 together with their standard deviations (σ) and the relations between both types of values (μ/σ) as measure for dispersion.

In contrast to Fig. 3, the semi-logarithmic diagrams in Fig. 4 attest differently dispersed data. Here the questions arise, if extreme outliers – such as in the diagram of the ratio of the average depth to the average width (d_{av5}/w_{av5}) – should not be discarded from the analyses and if the median might be more representative compared to the mean value (μ). To answer the first question, it can be argued that the highest points in the point cloud are generated by extremely wide but short rupture zones. To exclude them would require them to be discarded from the entirety of the statistical analyses to ensure consistent datasets. This, however, is wrong, since those landslides are not necessarily responsible for outliers in other diagrams; i.e., the same landslides might dispose of a normal ratio of the height between point 0 and point E to the maximum depth (H_{0E}/D). Datasets can, hence, not be individually depleted.

Concerning the median, it can be shown via several tests, that mean values (μ) and medians are usually very similar; therefore, both appear to be justifiable representatives. Due to the close link between the standard deviation (σ) and the mean value (μ), the latter seems more practical, however.

https://doi.org/10.5194/nhess-2019-240
Preprint. Discussion started: 18 September 2019

Natural Hazards and Earth System Sciences
Discussions

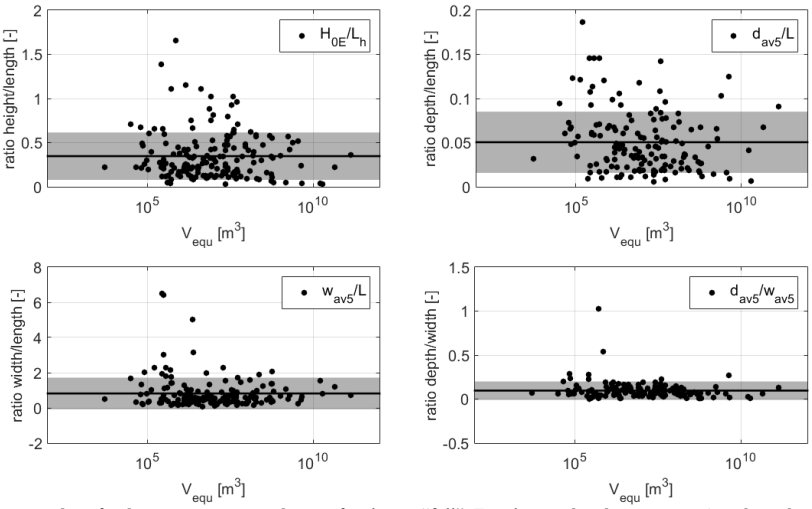

Fig. 4. Examples of volume–to–ratio correlations for the set "full". For shape-related parameters (i.e., here the ratios) the mean value (μ) is calculated. The shading indicates the symmetric belts of two standard deviations (±1σ) around the mean value (μ).

3. Discussion of results of all six sets

In contrast to the previous two subsections in which the analytical procedures and results were discussed with particular focus on the set "full", the discussion is dedicated to the comparison of results all six tested sets (Table 2).

In the first stage, it might be of interest how close regressions for individual parameters per set lie to each other. This question, indeed, concerns only dimension-related parameters whose values increase with greater calculated volumes (V_{equ}; Table 3a). To allow for easy comparison, regressions (Eq. (2)) for each dimension-related parameter per set are represented in a separate double-logarithmic diagram (colored lines in Fig. 5); based on the averages of the six constants (c) and the six factors (a) of the individual sets, average constants (c) and factors (a) that define these regressions are to be found in Table 5a (dashed black line in Fig. 5).

Exemplarily, Fig. 5 shows such regression comparisons for the maximum depth (D), the height between the point 0 and the point E (H_{0E}), the length along the slope (L) and the maximum width (W) in order to display one representative of each type of dimension-related parameters (i.e. depths, heights, lengths and widths). The diagrams reveal very good accordance between the regressions obtained for different sets due to very similar constants (c) and factors (a); the average regressions, thus, appear to be reliable representatives.

Moreover, a juxtaposition of the diagrams (Fig. 5) reveals that the regressions of depths are generally smaller than those of the heights and that the regressions of heights are smaller than those of the lengths and widths. Usually, landslide rupture zones are much higher than deep (Fig. 1). Also, the fact that lengths exceed heights seems logic, as – in the opposite case – the described setting would be rather atypical. The interesting detail within these magnitude comparisons is that on closer inspection, a difference emerges between lengths and widths, suggesting that landslide rupture zones are on average wider than long. This latter fact might have been overlooked as publications strive rather for the exact assessment of longitudinal cross sections (LCS) than for the one of the lateral extents (Domej, 2018). Probably, one of the reasons for this preferential focus is the so far predominant limitation of numerical landslide models to 2D. With the recent approaches of modeling landslides in 3D, their lateral extent becomes indispensable and, thus, the ellipticity defined by lengths and widths of a landslide might add important information.

Another – although rather visually subjective – feature is the zone of maximum overlap of the regressions of the six sets and the average regression. For depth parameters (D, d_0, d_1, d_2, d_3, d_E, d_{av5}, d_{av4} and d_{av3}) the regression overlap occurs between 10^6 m³ and 10^8 m³ of the calculated volume (V_{equ}), for height parameters (H_{0E} and H_{max}) between 10^7 m³ and 10^9 m³, and for length and width parameters between 10^8 m³ and 10^{10} m³. It seems, thus, that regressions of parameters with generally higher values tend to overlap better at higher ranges of the calculated volume (V_{equ}) and vice versa.

https://doi.org/10.5194/nhess-2019-240
Preprint. Discussion started: 18 September 2019

Natural Hazards and Earth System Sciences
Discussions

(a) V_{equ}/…	Average regression parameters (constant c | factor a)	(b) V_{equ}/…	Average horizontal reference line (μ | σ)	(c) V_{equ}/…	Average horizontal reference line (μ | σ)
D	-0.43 | 0.31	δ_0	50.15 | 19.65	H_{0E}/L_h	0.35 | 0.28
d_{av5}	-0.71 | 0.30	δ_1	18.65 | 13.85	H_{max}/L_h	0.36 | 0.27
d_{av4}	-0.61 | 0.30	δ_2	15.15 | 14.07	H_{0E}/W	0.49 | 0.51
d_{av3}	-0.52 | 0.31	δ_3	10.86 | 11.62	H_{0E}/w_{av5}	0.71 | 0.75
d_0	-	δ_E	-0.27 | 16.84	H_{0E}/w_{av3}	0.61 | 0.67
d_1	-0.49 | 0.31	cur	50.42 | 25.11	H_{0E}/D	3.99 | 3.25
d_2	-0.44 | 0.30	α_{equ}	18.10 | 12.01	H_{0E}/d_{av5}	7.90 | 5.82
d_3	-0.69 | 0.31	α_{lit}	20.75 | 12.86	H_{0E}/d_{av4}	6.32 | 4.65
d_E	-			H_{0E}/d_{av3}	4.91 | 3.58
H_{0E}	-0.02 | 0.32			D/L	0.10 | 0.07
H_{max}	-0.02 | 0.32			d_{av5}/L	0.05 | 0.03
L	0.40 | 0.35			d_{av4}/L	0.06 | 0.04
L_h	0.34 | 0.35			d_{av3}/L	0.08 | 0.05
W	0.31 | 0.35			W/L	1.22 | 1.47
w_{av5}	0.18 | 0.34			w_{av5}/L	0.84 | 0.89
w_{av3}	0.27 | 0.34			w_{av3}/L	0.97 | 1.00
w_0	0.00 | 0.32			D/W	0.14 | 0.12
w_1	0.25 | 0.34			D/w_{av5}	0.19 | 0.16
w_2	0.28 | 0.34			D/w_{av3}	0.16 | 0.14
w_3	0.25 | 0.34			d_{av5}/W	0.07 | 0.08
w_E	0.03 | 0.35			d_{av4}/W	0.09 | 0.09
				d_{av3}/W	0.11 | 0.12
				d_{av5}/w_{av5}	0.09 | 0.10
				d_{av3}/w_{av3}	0.13 | 0.14

Table 5a–c. Average results for the volume–to–parameter correlations (a, b) and for the volume–to–ratio correlations (c). For all dimension-related parameters (a), the regression parameters (constant c and factor a; Eq. 2) are given; for all shape-related parameters (b, c), the table shows the mean value (μ) with the respective standard deviation (σ). As d_0 contains 0 and d_E is always 0, they are not fitted in a double-logarithmic diagram.

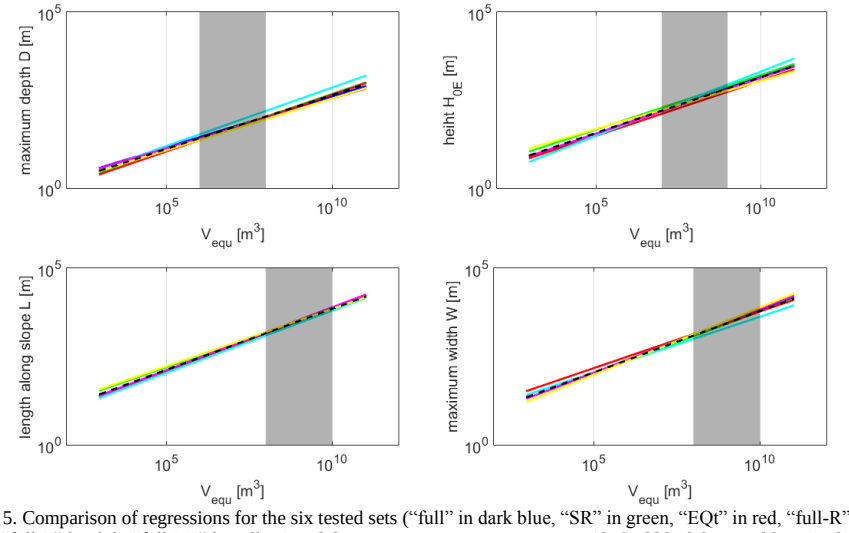

Fig. 5. Comparison of regressions for the six tested sets ("full" in dark blue, "SR" in green, "EQt" in red, "full-R" in light blue, "full-T" in pink, "full-RT" in yellow) and the respective average regression (dashed black line; Table 5a). The shading indicates the visually derived zone of maximum overlap.

In a second stage, it is of particular interest how similar mean values (μ) of individual shape-related parameters are throughout the six sets. Here, this question targets the analyses of the angles along the rupture surface (δ_0 to δ_E), the curvature (cur) and the slope angles (α_{equ} and α_{lit}) as well as the analyses of all ratios (Table 3b, Table 4).

https://doi.org/10.5194/nhess-2019-240
Preprint. Discussion started: 18 September 2019

Natural Hazards and Earth System Sciences
Discussions
Open Access
EGU

Because they are constant over the entire range of the calculated volume (V_{equ}) in addition to their similarity throughout the six tested sets (Table 2), the choice of the averages of the six mean values (μ) is a very legitimate representative value for each of the shape-related parameters (Table 5b–c). Expected shapes of landslide rupture zones based on the average ratios of dimension-related parameters are shown in Fig. 7.

In Domej et al. (2017), the ratio of the height between the point 0 and the point E to the projected length (H_{0E}/L_h), the ratio of the average depth to the length along the slope (d_{av5}/L), the ratio of the average width to the projected length along the slope (w_{av5}/L_h) and the ratio of the average depth to the average width (d_{av5}/w_{av5}) were evaluated for three sets ("full", "SR" and "EQt") via a grouping approach (Fig. 2a). The hereby obtained ratios (Fig. 6a–d, Table 6) match those of the here presented analyses surprisingly well.

Ratios in Domej et al. (2017)	Group 10^3–10^6 m³	Group 10^6–10^9 m³	Group 10^9–10^{12} m³	Average per set
H_{0E}/L_h	0.34 [a] 0.38 [b] 0.29 [c]	0.33 [a] 0.35 [b] 0.29 [c]	0.25 [a] 0.32 [b] 0.23 [c]	**0.31** [a] **0.35** [b] **0.27** [c]
d_{av5}/L	0.05 [a] 0.05 [b] 0.05 [c]	0.04 [a] 0.04 [b] 0.03 [c]	0.05 [a] 0.06 [b] 0.06 [c]	**0.05** [a] **0.05** [b] **0.05** [c]
w_{av5}/L	0.85 [a] 0.60 [b] 1.48 [c]	0.63 [a] 0.58 [b] 0.80 [c]	0.89 [a] 0.83 [b] 0.91 [c]	**0.79** [a] **0.67** [b] **1.06** [c]
d_{av5}/w_{av}	0.07 [a] 0.09 [b] 0.04 [c]	0.07 [a] 0.07 [b] 0.04 [c]	0.06 [a] 0.08 [b] 0.07 [c]	**0.07** [a] **0.08** [b] **0.05** [c]

Table 6. Ratios per volume group, as reported in Domej et al. (2017). The value triplets correspond to the ratios per tested set ("full" ([a]), "SR" ([b]) and "EQt" ([c])).

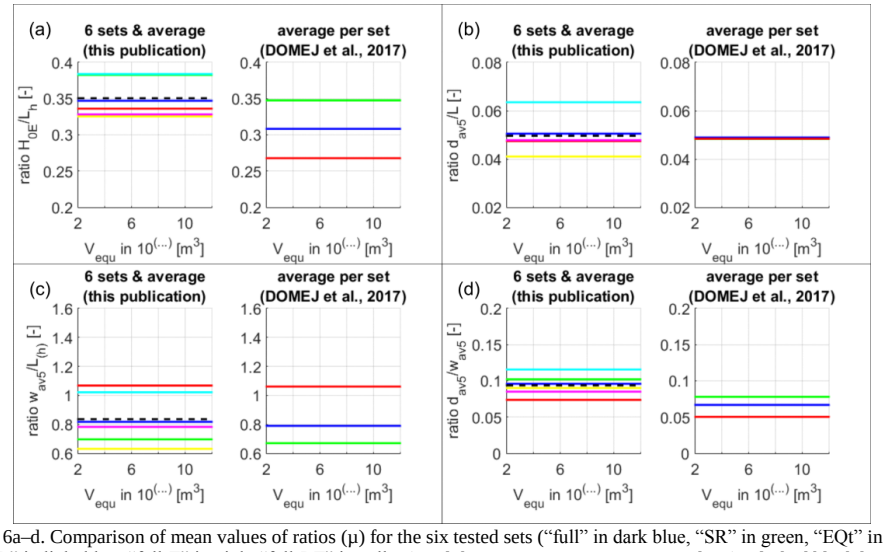

Fig. 6a–d. Comparison of mean values of ratios (μ) for the six tested sets ("full" in dark blue, "SR" in green, "EQt" in red, "full-R" in light blue, "full-T" in pink, "full-RT" in yellow) and the respective average mean value (μ; dashed black line) and for the average of the mean values (μ) per set ("full" in dark blue, "SR" in green, "EQt" in red) as presented in Domej et al. (2017; right subplots; Table 6).

https://doi.org/10.5194/nhess-2019-240
Preprint. Discussion started: 18 September 2019

Natural Hazards and Earth System Sciences
Discussions

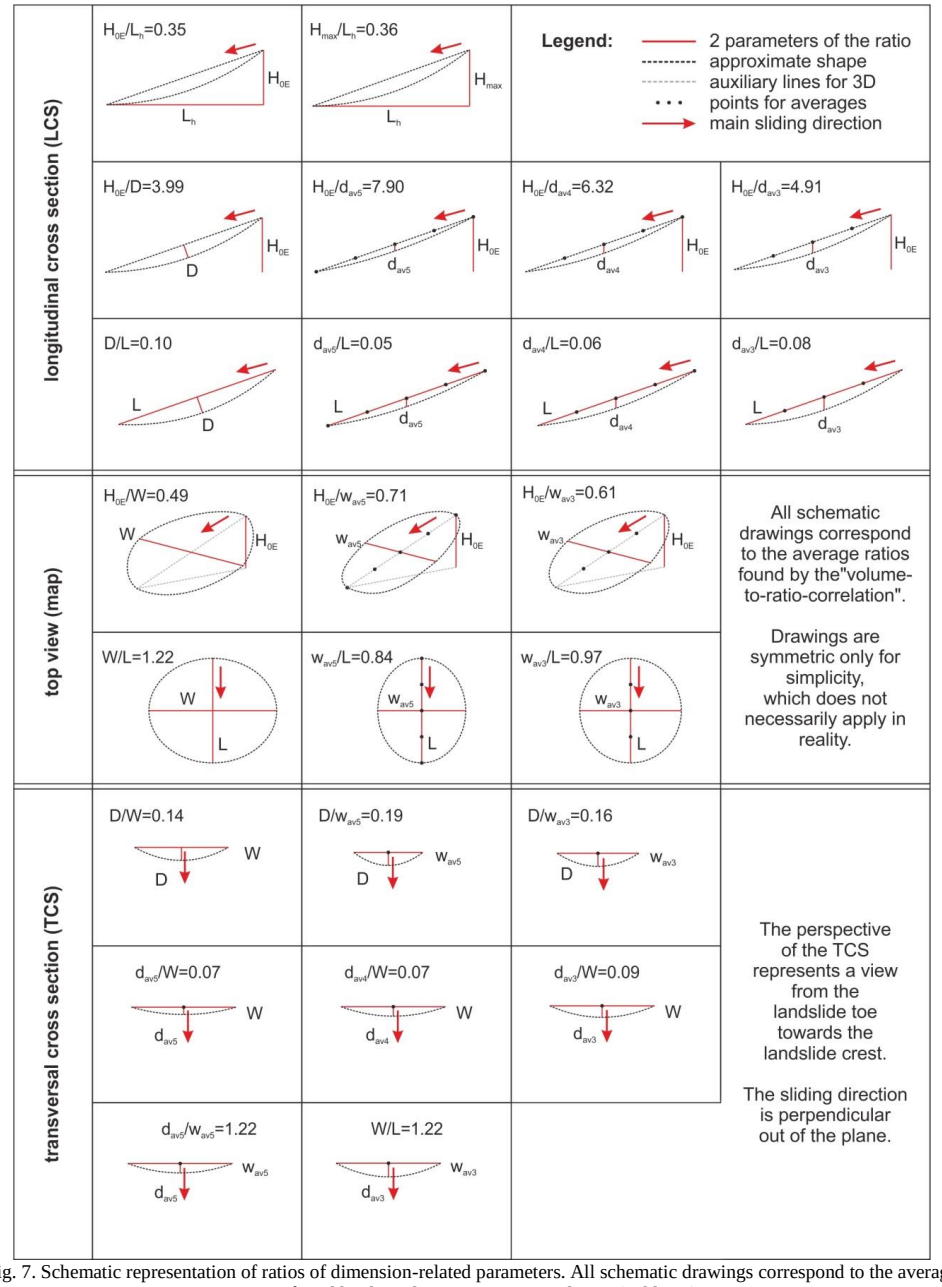

Fig. 7. Schematic representation of ratios of dimension-related parameters. All schematic drawings correspond to the average ratios found by the volume–to–ratio-correlation (Table 5c).

4. Conclusion and perspectives

In this work, the newly built, chronological and global landslide database presented by Domej et al. (2017) was revisited with the aim of a more detailed exploration of the statistical behavior of dimension- and shape-related parameters characterizing a landslide rupture zone in 3D (Fig. 1, Table 1). Domej et al. (2017) revealed a significant difference in the statistical behavior of these two types of parameters. Via a tripartite grouping approach of parameters with respect to their calculated volume (V_{equ}) all dimension-related parameters showed a

https://doi.org/10.5194/nhess-2019-240
Preprint. Discussion started: 18 September 2019

Natural Hazards and Earth System Sciences
Discussions
Open Access
EGU

clear increase with greater calculated volumes (V_{equ}), whereas all shape-related parameters and the ratios of dimension-related parameters remained constant throughout the full range of calculated volumes (V_{equ}).

The here presented analyses are carried out without grouping (Fig. 2b) and with many more parameters of both types in order to refine and improve the results of Domej et al. (2017). For six different sets (Table 2), that were filtered from the landslide database, the analyses are based on volume–to–parameter correlations of all exploitable dimension-related parameters (i.e. depths, heights, lengths, and widths) and the eight shape-related parameters (i.e. angles along rupture surface (δ_0 to δ_E), curvature (cur), and reported and calculated slope angle (α_{equ} and α_{lit})) as well as on volume–to–ratio correlations of all ratios of dimension-related parameters.

From the first type of correlation, one can confirm the overall result of Domej et al. (2017) – however, with much greater detail, which also allows for a broader spectrum of use. Since regressions for dimension-related parameters are very similar (Fig. 5, Table 5a) one could use the average regression of a distinct parameter to extrapolate from a given value to the calculated volume (V_{equ}) of a landslide. This potential field of an application might be of interest for preliminary assessments of rupture zone dimensions, e.g., during fieldwork or rapid first stage inventories anticipating exact geological, geotechnical and geophysical surveys. Depending on the desired accuracy, one might consider the average regressions per respective dimension-related parameter or one of the set specific regressions can be used if the considered landslide is known to match one of the filters (Table 5a).

As for the shape-related parameters, the analyses also delivers very satisfactory results compared to those of Domej et al. (2017) with those ratios existing in both publications being almost identical (Fig. 6a–d, Table 6, Table 5c). Again, this publication offers a much wider range of possible application since all eight shape-related parameters, and many more ratio combinations were considered. On the one hand, one might benefit here from the finding that the eight shape-related parameters (i.e., angles along rupture surface (δ_0 to δ_E), curvature (*cur*), and reported and calculated slope angle (α_{equ} and α_{lit})) are stable throughout all volume ranges – a fact that also finds its application during preliminary assessments of rupture zone dimensions. On the other hand, one might make use of the constancy of ratios of dimension-related parameters by deducing one of the two parameters when the other one is given. Especially this latter aspect seems to be promising for remote sensing surveys when initial rupture areas or rupture volumes should be delineated. Very often, remote sensing allows for mapping of entire landslide areas that are affected by the sliding process (Fig. 8a–d). Here, it could remain unclear where the rupture zone ends due to overlaps or even offsets of landslide deposits. If in such cases, dimension-related parameters relating to horizontal and/or vertical expansion are known, and if one relies on constant ratios between them, it could be possible to trace back the rupture areas and/or the rupture volumes of landslides.

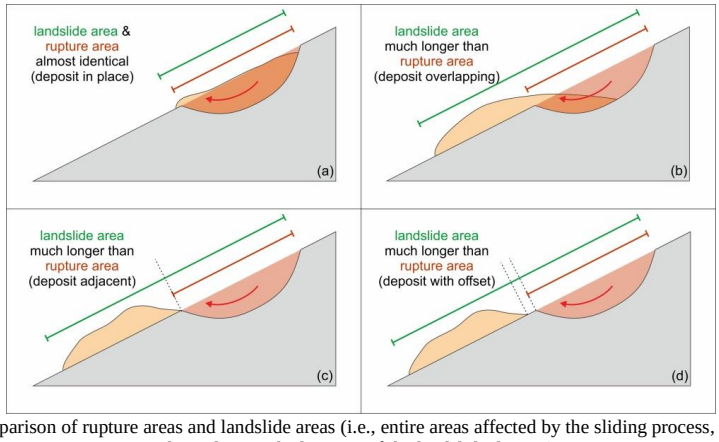

Fig. 8a–d. Comparison of rupture areas and landslide areas (i.e., entire areas affected by the sliding process, which is mainly dependent on the location of the landslide deposit).

As a final remark on perspectives, it should be mentioned that – although the entire statistical analyses were carried out based on the calculated volume (V_{equ}) as first correlation parameter for the volume–to–parameter correlations as well as the for the volume–to–ratio correlations – it is possible to filter data with respect to different correlation parameters at any moment. It exists, therefore, an almost countless number of options to retrieve and analyze data from the landslide database. According to different needs and demands, filters can be customized, and it is likewise possible to create new parameters or ratios from the existing dimension- and/or shape-related parameters.

https://doi.org/10.5194/nhess-2019-240
Preprint. Discussion started: 18 September 2019

Natural Hazards and Earth System Sciences
Discussions

Data sources

Data included in the database does not belong to the authors of this article. The following references do not include publications associated with the individual landslides in the database. However, it is possible to provide (on demand) a full list of evaluated literature for every case.

Competing interests

The authors declare that they have no conflict of interest.

References

Bird, J. F., Bommer, J. J.: Earthquake losses due to ground failure, Eng. Geol., 75/2, 147–179, https://doi.org/10.1016/j.enggeo.2004.05.006, 2004.

Bucknam, R. C., Coe, J. A., Chavarria, M. M., Godt, J. W., Tarr, A. C., Bradley, L. A., Rafferty, S., Hancock, D., Dart, R. L., and Johnson, M. L.: Landslides Triggered by Hurricane Mitch in Guatemala – Inventory and Discussion, U.S. Geol. Surv., Denver, USA, Open File Rep. 01-443, 40 pp., 2001.

Cardinali, M., Ardizzone, F., Galli, M., Guzzetti, F., and Reichenbach, P.: Landslides triggered by rapid snow melting: the December 1996 – January 1997 event in Central Italy, in: Mediterranean Storms, Proceedings of the 1st Plinius Conference, Maratea, Italy, 14–16 October 1999, 439–448, 2000.

Cruden D. M. and Varnes D. J.: Landslide types and processes, in: Landslides: Investigation and Mitigation, edited by: Turner, A. K. and Schuster, R. L., National Research Council, Transportation Research Board, Washington D. C., USA, Special Rep. 247, 36–75, 1996.

Domej, G.: Seismically induced effects and slope stability in urbanized zones by numerical modeling, Ph.D. thesis, Institut Français des Sciences et Technologies des Transports, de l'Aménagement et des Réseaux, Université Paris–Est, France, 266 pp., 2018.

Domej, G., Bourdeau, C., Lenti, L., Martino, S., and Pluta K.: Mean landslide geometries inferred from a global database of earthquake– and non–earthquake–triggered landslides, Italian Journal of Engineering Geology and the Environment, 17/2, 87–107, https://doi.org/10.4408/IJEGE.2017-02.O-05, 2017.

Froude, M. J. and Petley, D. N.: Global fatal landslide occurrence from 2004 to 2016, Nat. Hazards Earth Syst. Sci., 18, 2161–2181, https://doi.org/10.5194/nhess-18-2161-2018, 2018.

Harp, E. L. and Jibson, R. L.: Inventory of landslides triggered by the 1994 Northridge, California earthquake. U.S. Geol. Surv., Denver, USA, Open File Rep. 95-213, 17 pp., 1995.

Harp, E. L. and Jibson, R. L.: Landslides triggered by the 1994 Northridge, California earthquake, Bull. Seismol. Soc. Am., 86/1B, S319–S332, 1996.

Keefer, D. K.: Landslides caused by earthquakes, Geol. Soc. Am. Bull., 95/4, 406–421, 1984.

Lott, N., McCown, S., Graumann, A., Ross, T., and Lackey M.: Hurricane Mitch 1999 – The deadliest Atlantic hurricane since 1780. National Climatic Data Center of the National Oceanic and Atmospheric Administration, Asheville, USA, 10 pp., available at: ftp://ftp.ncdc.noaa.gov/pub/data/extremeevents/specialreports/Hurricane-Mitch-1998.pdf, last access: 30 June 2019, 1999.

Malamud B. D, Turcotte D. L., Guzzetti F., and Reichenbach P.: Landslide inventories and their statistical properties, Earth Surf. Processes Landforms, 29, 687–711, https://doi.org/10.1002/esp.1064, 2004.

Prestininzi A. and Romeo R., Earthquake–induced ground failures in Italy, Eng. Geol., 58/3–4, 387–397, https://doi.org/10.1016/S0013-7952(00)00044-2, 2000.

Rodríguez, C. E., Bommer, J. J., and Chandler, R. J.: Earthquake-induced landslides: 1980–1997, Soil Dyn. Earthquake Eng., vol. 18/5, p. 325–346, https://doi.org/10.1016/S0267-7261(99)00012-3, 1999.

Schlögel, R., Torgoev, I., De Marneffe, C., and Havenith, H. B.: Evidence of a changing size–frequency distribution of landslides in the Kyrgyz Tien Shan, Central Asia, Earth Surf. Processes Landforms, 36/12, 1658–1669, https://doi.org/10.1002/esp.2184, 2011.

Tanyaş, H., Van Westen, C. J., Allstadt, K. E., Nowicki Jessee, M. A., Görüm, T., Jibson, R.W., Godt J. W., Sato, H. P., Schmitt, R. G., Marc, O., and Hovius, N.: Presentation and Analysis of a Worldwide Database of Earthquake–Induced Landslide Inventories, J. Geophys. Res., 122/10, 1991–2015, https://doi.org/10.1002/2017JF004236, 2017.

USGS: Landslide types and processes. U.S. Geol. Surv., Denver, USA, Fact Sheet 2004-3072, 4 pp., 2004.

Varnes, D. J.: Slope movement types and processes, in: Landslides – Analysis and Control, edited by: Schuster, R. L. and Krizek, R. J., National Research Council, Transportation Research Board, Washington D. C., USA, Special Rep. 176, 11–33, 1978.

Yin, Y. P., Wang, F. W., and Sun, P.: Landslide hazards triggered by the 2008 Wenchuan earthquake, Sichuan, China, Landslides, 6/2, 139–151, https://doi.org/10.1007/s10346-009-0148-5, 2009.